ADVANCED ENERGY MATERIALS

# Supporting Information

for *Adv. Energy Mater.,* DOI: 10.1002/aenm.201803436

## Realizing Three-Electron Redox Reactions in NASICON-Structured $Na_3MnTi(PO_4)_3$ for Sodium-Ion Batteries

*Ting Zhu, Ping Hu, Xuanpeng Wang, Zhenhui Liu, Wen Luo, Kwadwo Asare Owusu, Weiwei Cao, Changwei Shi, Jiantao Li, Liang Zhou,* and Liqiang Mai**

# Supporting Information

**Realizing Three-Electron Redox Reactions in NASICON-Structured $Na_3MnTi(PO_4)_3$ for Sodium-ion Batteries**

Ting Zhu,[a] Ping Hu,[a] Xuanpeng Wang,[a] Zhenhui Liu,[a] Wen Luo,[a] Kwadwo Asare Owusu,[a] Weiwei Cao,[b] Changwei Shi,[a] Jiantao Li,[a] Liang Zhou,[a]* and Liqiang Mai[a]*

[a] T. Zhu, P. Hu, X. P. Wang, Z. H. Liu, Dr. W. Luo, K. A. Owusu, C. W. Shi, J. T. Li, Prof. L. Zhou, Prof. L. Q. Mai
State Key Laboratory of Advanced Technology for Materials Synthesis and Processing
Wuhan University of Technology, Wuhan 430070, P. R. China
[b] W. W. Cao
UPR3079 CEMHTI, 1D Avenue de la Recherche Scientifique, 45071 Orléans Cedex2, France

E-mail: liangzhou@whut.edu.cn, mlq518@whut.edu.cn

**Synthesis of soft carbon**

The soft carbon was prepared by direct pyrolysis of 3,4,9,10-perylene tetracarboxylic dianhydride (Alfa Aesar 98%) at 900 °C for 10 h in Ar (5 °C $min^{-1}$).

**Full cell electrochemical performance test**

The NMTP/C-650 cathode was further assembled with the soft carbon anode to obtain NMTP/C-650//C full cells. Before the full cell test, the soft carbon based anode was cycled at 100 mA $g^{-1}$ for 6 cycles. Electrochemical performance of the NMTP/C-650//C full cells was measured with a voltage window of 0.5 – 4.2 V.

**Calculation of the theoretical capacity of $Na_3MnTi(PO_4)_3$**

The intercalation/deintercalation number for each mol of $NaMnTi(PO_4)_3$ (the first charged state), 3 mol of $Na^+$ can be stored.

Theoretical capacity of $Na_3MnTi(PO_4)_3$:

$$(3 \text{ mol} * 96500 \text{ C/mol}) / (456.7 \text{ g/mol} * 3.6 \text{ C/mAh}) = 176 \text{ mAh g}^{-1} \quad (1)$$

**Table S1**. Detailed structural information of $Na_3MnTi(PO_4)_3$ derived from Rietveld Refinement.

| | | |
|---|---|---|
| Space group=R-3c | $R_p$ = 2.39 % | $R_{wp}$ = 3.42 % |
| a (Å) = 8.8343 | c (Å) = 21.6654 | a/b = 1.0000 |
| b/c = 0.4078 | c/a = 2.4524 | V(Å$^3$) = 1464.35 |

| Atom | Wyckoff site | X | Y | Z |
|---|---|---|---|---|
| Na(1) | 6b | 0.00000 | 0.00000 | 0.00000 |
| Na(2) | 18e | 0.63275 | 0.00000 | 0.2500 |
| Mn(1) | 12c | 0.00000 | 0.00000 | 0.14860 |
| Ti(1) | 12c | 0.00000 | 0.00000 | 0.14860 |
| P(1) | 18e | 0.29857 | 0.00000 | 0.2500 |
| O(1) | 36f | 0.20040 | 0.17431 | 0.09417 |
| O(2) | 36f | 0.01858 | 0.21265 | 0.19197 |

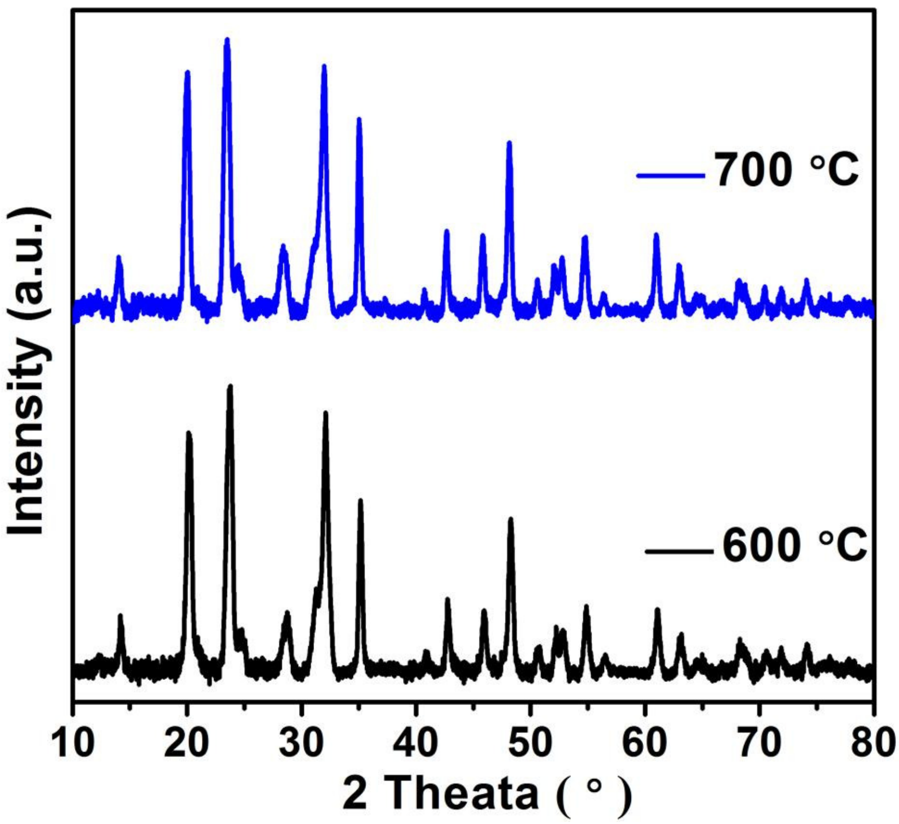


**Figure S1.** XRD patterns of NMTP/C-600 and NMTP/C-700.

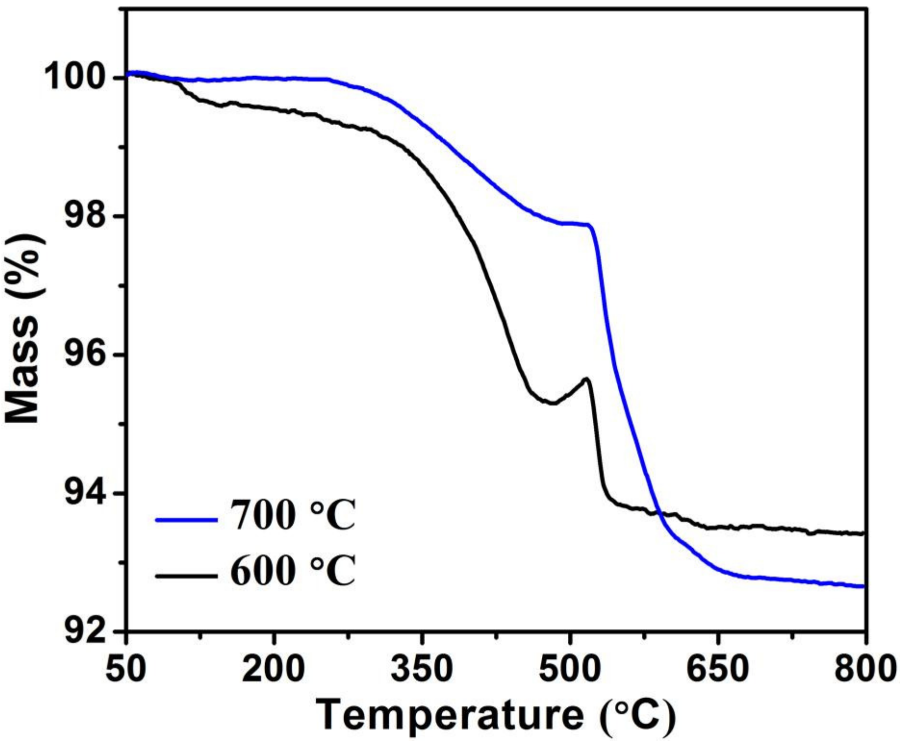


**Figure S2.** TGA curves of NMTP/C-600 and NMTP/C-700.

**Table S2.** CHNS analysis results of the NMTP/C-600, NMTP/C-650, and NMTP/C-700.

| Sample | Chemical composition (wt.%) | | |
|---|---|---|---|
| | C | H | N |
| NMTP/C-600 | 7.49 | 0 | 0.26 |
| NMTP/C-650 | 8.85 | 0 | 0.27 |
| NMTP/C-700 | 6.59 | 0 | 0.18 |

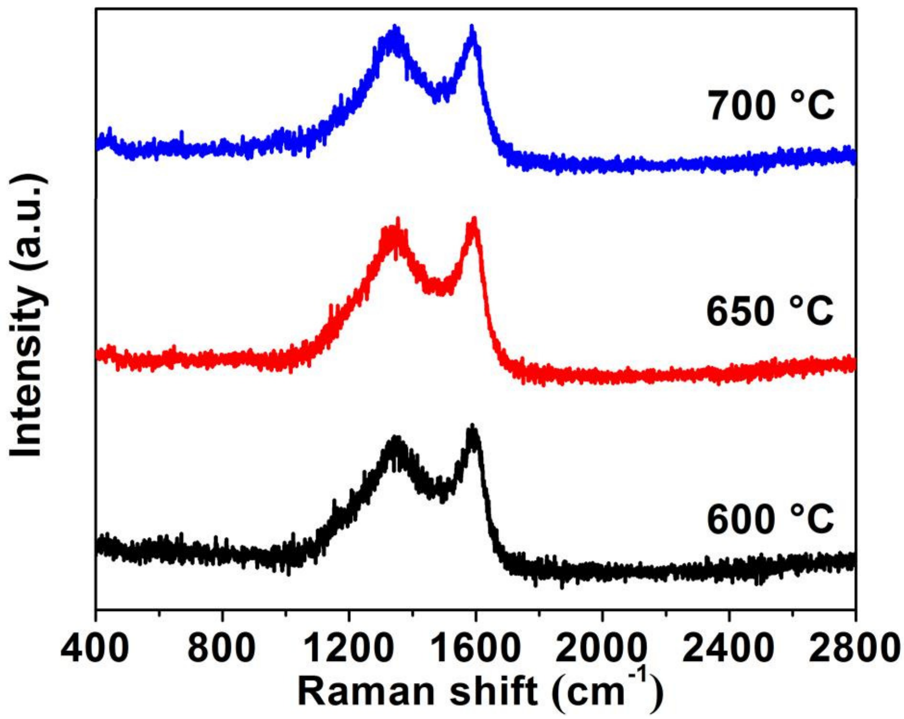


**Figure S3.** Raman spectra of the NMTP/C-600, NMTP-650, and NMTP/C-700.

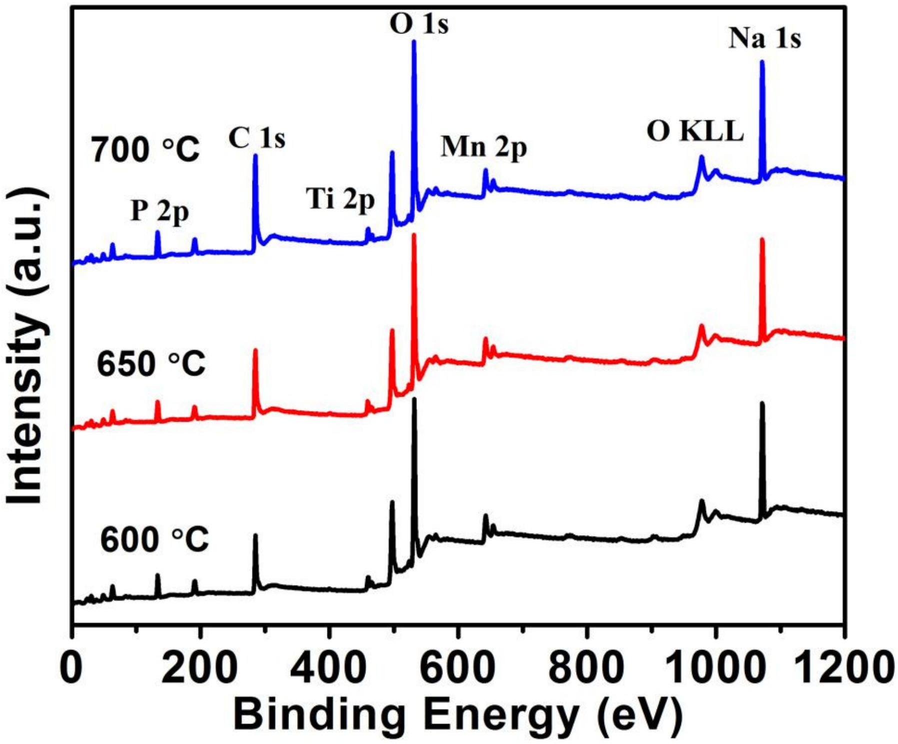


**Figure S4.** XPS survey spectra of the NMTP/C-600, NMTP-650, and NMTP/C-700.

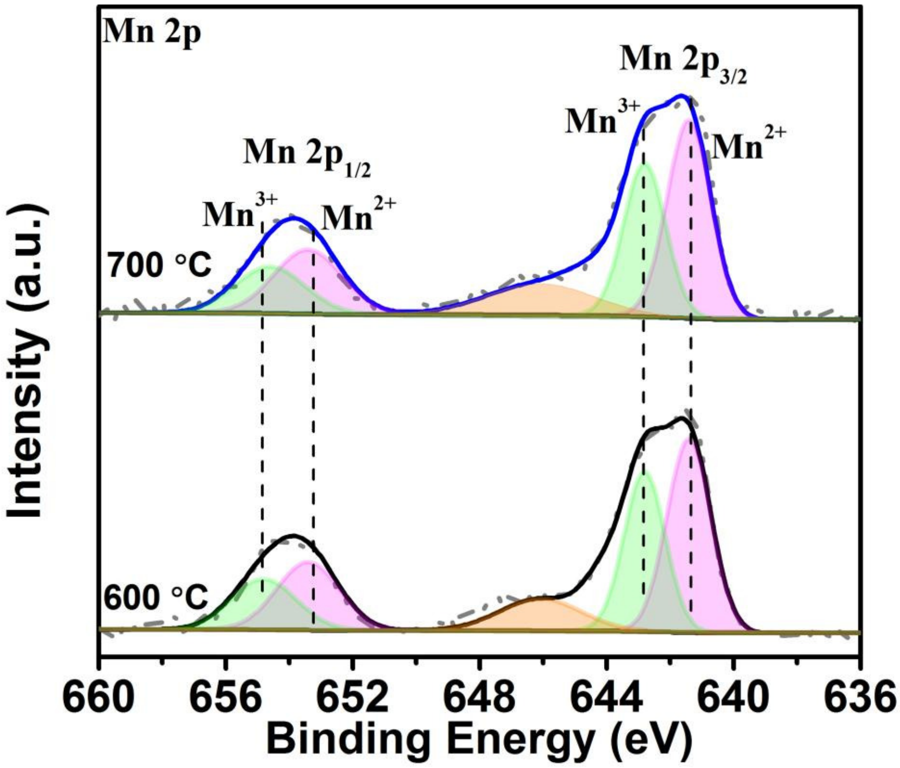


**Figure S5.** High-resolution Mn 2p XPS spectra of NMTP/C-600 and NMTP/C-700.

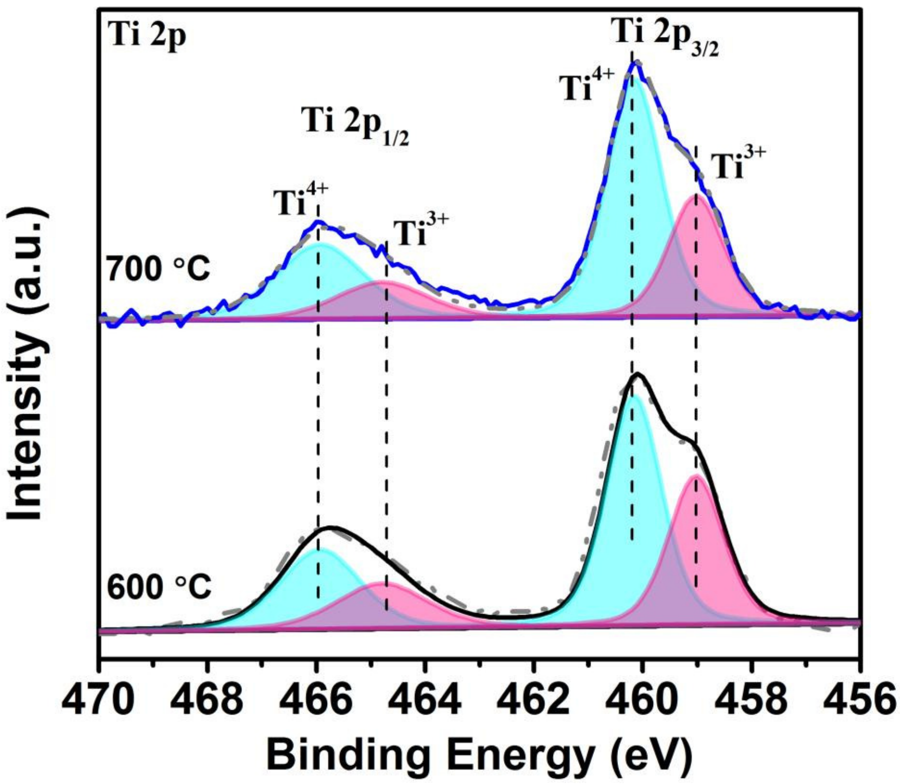


**Figure S6.** High-resolution Ti 2p XPS spectra of NMTP/C-600 and NMTP/C-700.

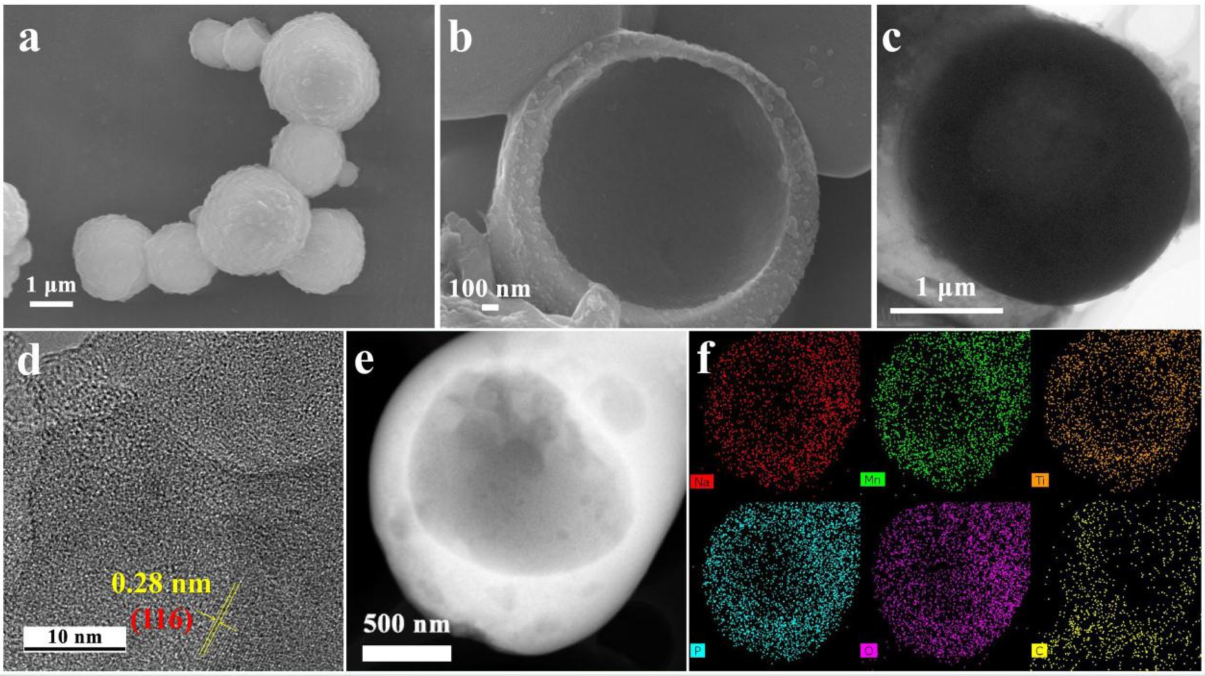


**Figure S7.** SEM images (a, b), TEM images (c), and HRTEM image (d) of NMTP/C-600; HAADF-STEM image (e) of NMTP/C-600 and the corresponding elemental mappings (f) of manganese (green), titanium (orange), carbon (yellow), sodium (red), oxygen (purple), and phosphorus (blue).

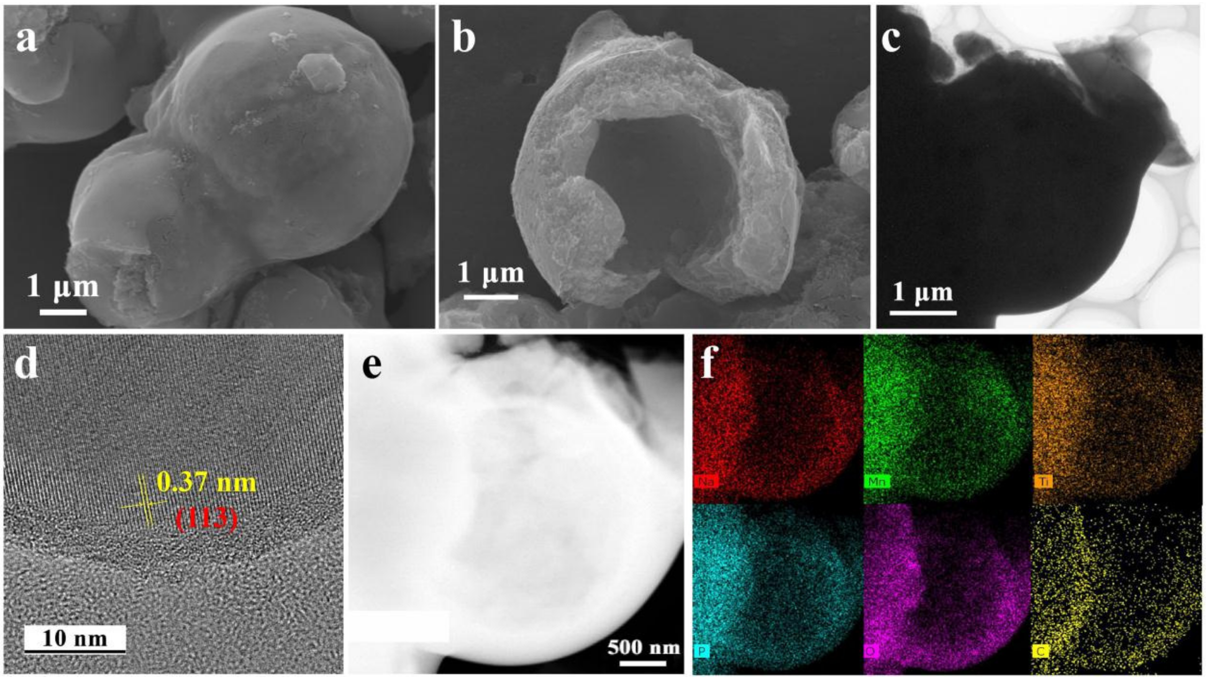


**Figure S8.** SEM images (a, b), TEM images (c), and HRTEM image (d) of NMTP/C-700; HAADF-STEM image (e) of NMTP/C-700 and the corresponding elemental mappings (f) of manganese (green), titanium (orange), carbon (yellow), sodium (red), oxygen (purple), and phosphorus (blue).

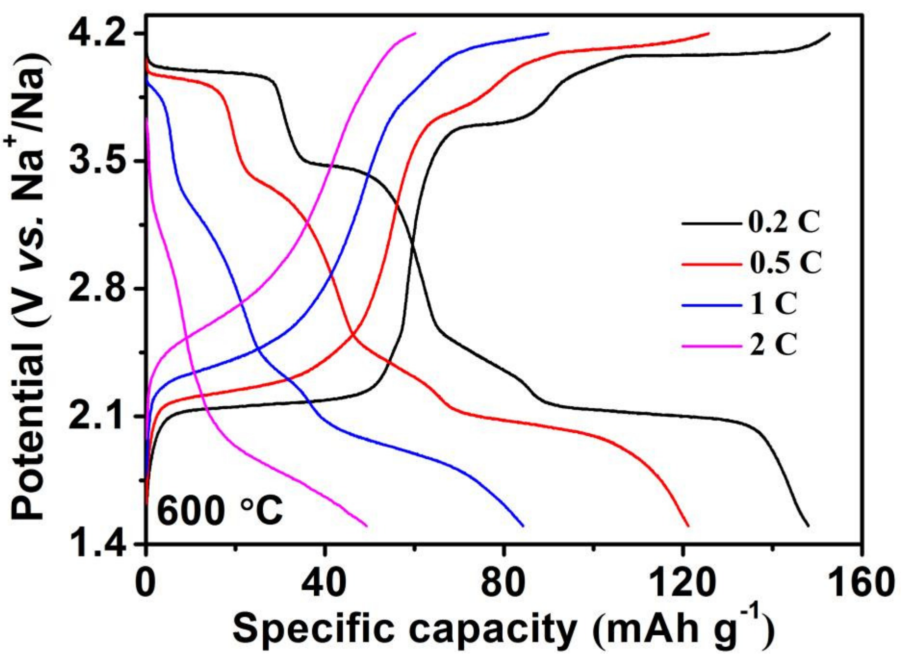


**Figure S9.** Charge/discharge curve of NMTP/C-600 at different rates.

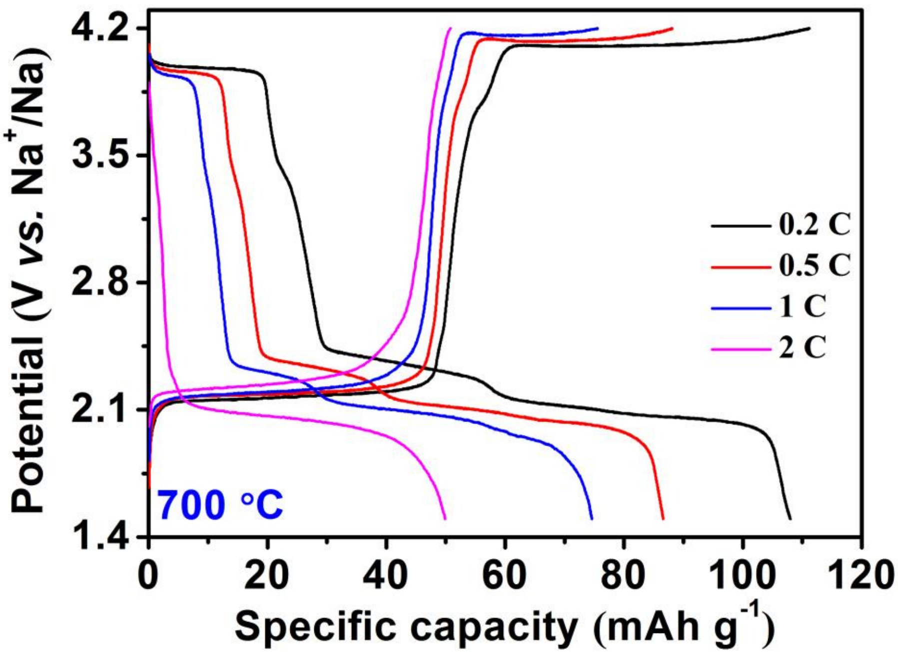


**Figure S10.** Charge/discharge curve of NMTP/C-700 at different rates.

**Table S3.** Electrochemical performances of recently reported NASICON-based sodium-ion battery cathode materials

| **Materials** | **Theoretical capacity (x mAh g$^{-1}$)** | **Voltage range** | **Specific capacity at y C** | **Capacity retention after n cycle at z C** | **Reference** |
|---|---|---|---|---|---|
| **$Na_3MnTi(PO_4)_3$@C** | **176** | **1.5 - 4.2 V** | **160 (y=0.2)** | **92% (n=500, z=2)** | **This Work** |
| $Na_3V_2(PO_4)_3$ | 118 | 2.5 - 4.2 V | 117 (y = 1) | 92% (n=500, z=5) | 1 |
| $Na_3Fe_2(PO_4)_3$ | 115 | 1.5 - 4.2 V | 109 (y=0.1) | 96% (n=200, z=1) | 2 |
| $Na_3MnTi(PO_4)_3$ | 117 | 2.5 - 4.2 V | 114 (y=0.1) | 77% (n=100, z=0.1) | 3 |
| $Na_{3+x}V_{2-x}Ni_x(PO_4)_3$/C | 118 | 2.5 - 4 V | 113 (y=0.2) | 95% (n=100, z=1) | 4 |
| $Na_3FeV(PO_4)_3$ | 116 | 2.5 - 3.8 V | 103 (y=1) | 95% (n=1000, z=1) | 5 |
| $Na_4MnV(PO_4)_3$ | 117 | 2.5 - 3.8 V | 101 (y=1) | 89% (n=1000, z=1) | 5 |
| $Na_4NiV(PO_4)_3$ | 116 | 2.5 - 4.2 V | 80 (y=1) | 83% (n=1000, z=1) | 5 |
| $Na_4MnV(PO_4)_3$@C@GA | 117 | 2.5 - 3.8 V | 107 (y=1) | 69% (n=4000, z=20) | 6 |
| $Na_3Cr_2(PO_4)_3$ | 117 | 2.5 - 4.7 V | 98 (y=0.5) | 6% (n=20, z=0.5) | 7 |

**References**

**S1.** Y. N. Xu, Q. L. Wei, C. Xu, Q. D. Li, Q. Y. An, P. F. Zhang, J. Z. Sheng, L. Zhou, L. Q. Mai, Adv. Energy Mater. **2016**, 6, 1600389.

**S2.** R. Rajagopalan, B. Chen, Z. C. Zhang, X. L. Wu, Y. H. Du, Y. Huang, B. Li, Y. Zong, J. Wang, G. H. Nam, M. Sindoro, S. X. Dou, H. K. Liu, H. Zhang, Adv. Mater. **2017**, 29, 1605694.

**S3.** H. C. Gao, Y. T. Li, K. Park, J. B. Goodenough, Chem. Mater. **2016**, 28, 6553.

**S4.** H. Li, Y. Bai, F. Wu, Q. Ni, C. Wu, ACS Appl. Mater. Interfaces **2016**, 8, 27779.

**S5.** W. D. Zhou, L. G. Xue, X. J. Lü, H. C. Gao, Y. T. Li, S. Xin, G. T. Fu, Z. M. Cui, Y. Zhu, J. B. Goodenough, Nano Lett. **2016**, 16, 7836.

**S6.** H. X. Li, T. Jin, X. B. Chen, Y. Q. Lai, Z. A. Zhang, W. Z. Bao, L. F. Jiao, Adv. Energy Mater. **2018**, 1801418.

**S7.** K. Kawai, W. W. Zhao, S. Nishimura, A. Yamada, ACS Appl. Energy Mater. **2018**, 1, 928.

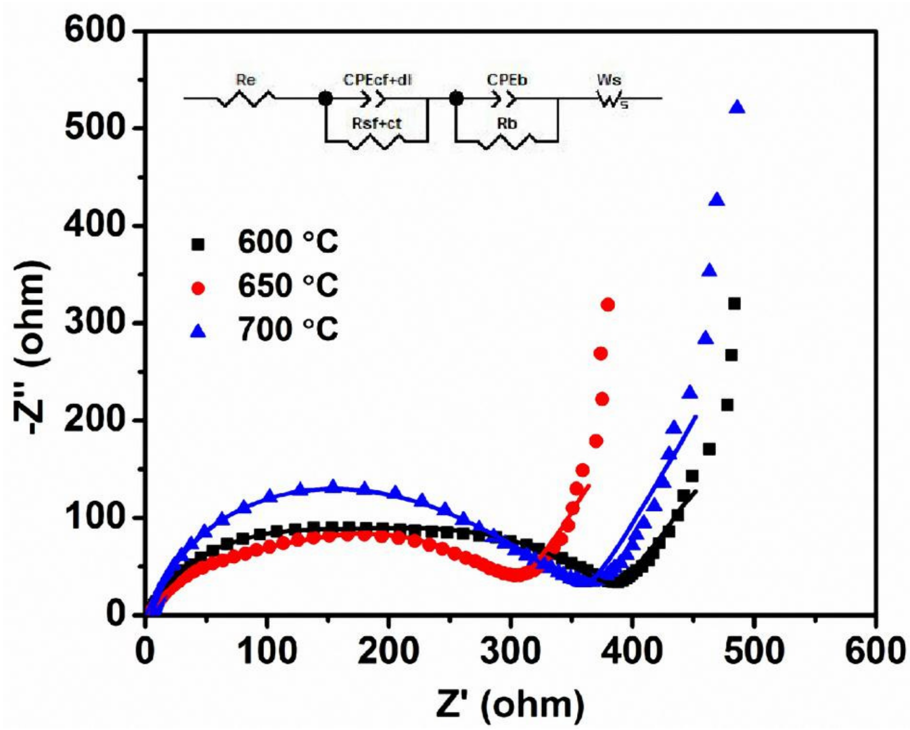


**Figure S11.** Nyquist plots of NMTP/C-600, NMTP/C-650, and NMTP/C-700. (inset: equivalent circuit model. $R_e$ represents electrolyte resistance, $R_{sf+ct}$ represents surface and charge transfer resistance, $R_b$ represents bulk resistance, CPE represents constant phase element, and W represents Warburg impedance).

**Table S4.** Fitting results of the EIS plots.

| Sample | $R_{sf+ct}$/Ω | $R_b$/Ω |
|---|---|---|
| NMTP/C-600 | 141.5 | 237.3 |
| NMTP/C-650 | 88.39 | 208.4 |
| NMTP/C-700 | 157.8 | 196.9 |

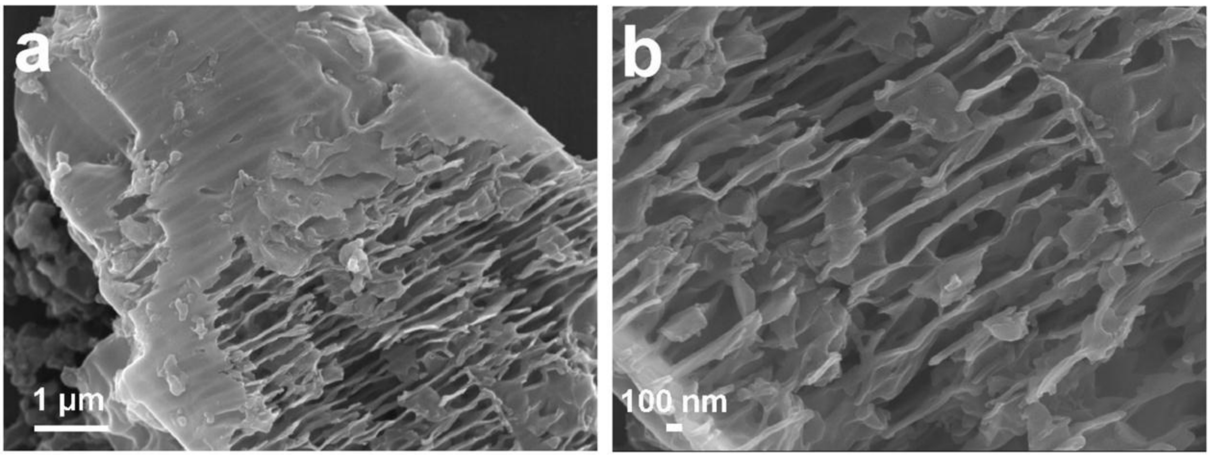


**Figure S12.** SEM images of soft carbon.

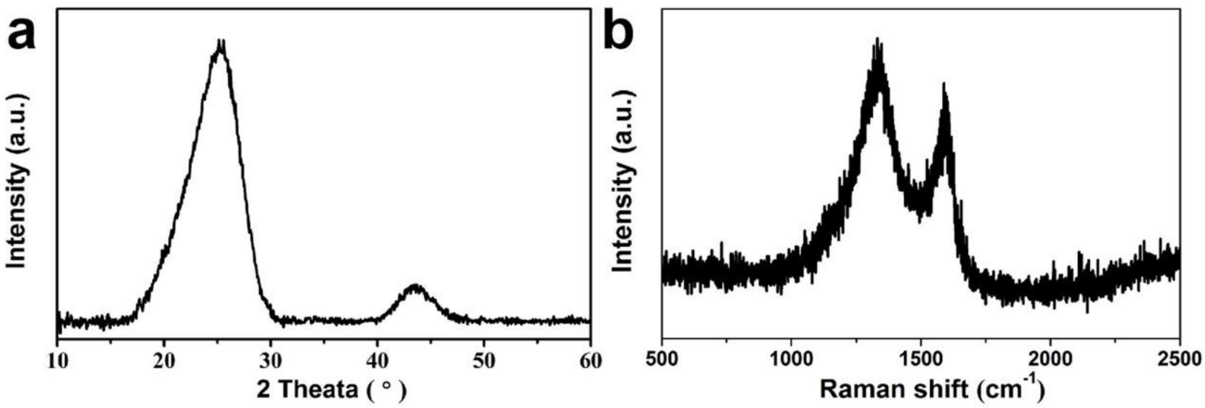


**Figure S13.** XRD pattern (a) and Raman spectrum (b) of soft carbon.

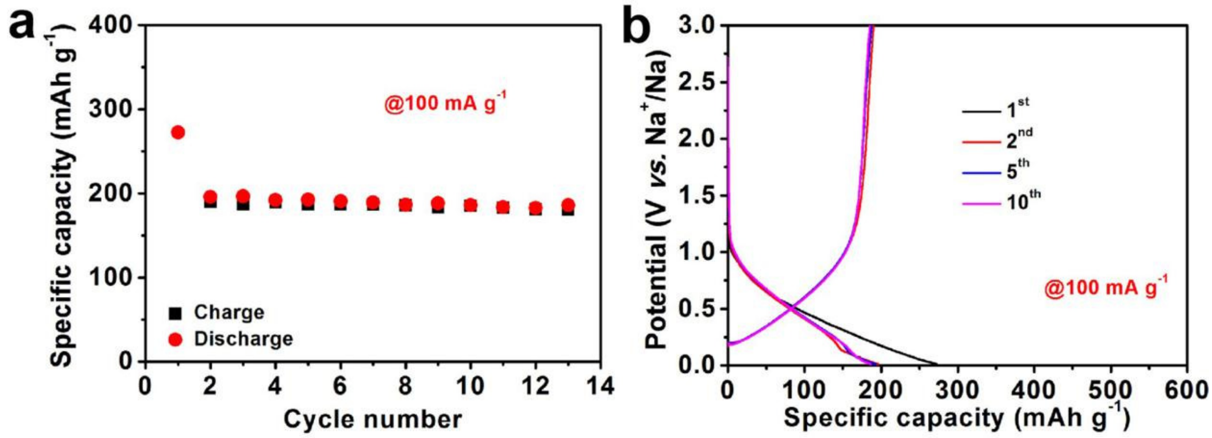


**Figure S14.** The cyclic performance (a) and charge/discharge curves (b) of soft carbon tested at 100 mA $g^{-1}$.

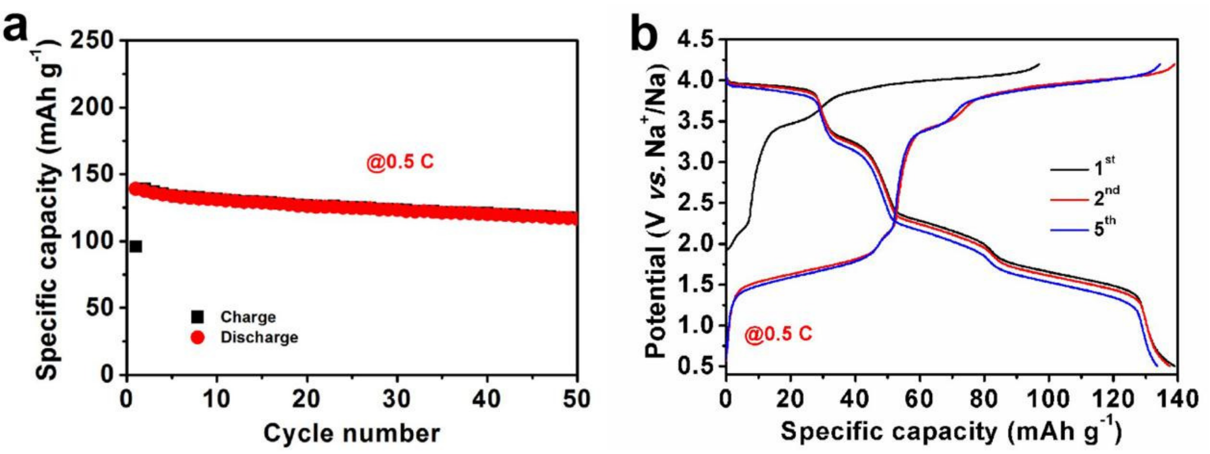


**Figure S15.** The cycling performance (a) and charge/discharge curves (b) of NMTP/C-650//C at 0.5 C.